

Testing and Modeling of Nonlinear Properties of Shock Absorbers for Vehicle Dynamics Studies

Yan Cui, Thomas R. Kurfess, and Michael Messman

Abstract—The objective of this work is to develop a new testing and analysis methodology to obtain the nonlinear characteristics of an automotive shock absorber. The front shock absorber on a Mazda CX-7 was tested on the single-post shaker test bench. The shock absorber piston velocity test range is between 0.01m/s and 1.3m/s, corresponding to typical velocities of a vehicle suspension generated by road irregularities. Three shock absorber models were built and validated using experimental shock absorber data. The power function model and polynomial model accurately capture the nonlinear characteristics of a shock absorber and can be quickly fit to experimental data for use in vehicle simulations. The influence of the shock absorber models on vehicle dynamics in vertical direction was analyzed.

Index Terms—shock absorber, nonlinearity, vehicle dynamics.

I. INTRODUCTION

A key aspect of vehicle research is improving ride quality and handling performance. Target comfort and handling performance can be achieved through analysis and modification of the vehicle and modification of its subsystems such as the electronic stability control and the suspension controller [1,2,3]. These control systems operate by comparing vehicle dynamic behavior to a pre-determined mathematical vehicle model. Therefore, high fidelity mathematical models that accurately capture the dynamics of the vehicle suspension system and predict the vehicle behavior are critical.

A key element in any vehicle suspension system is the shock absorber. It plays a vital role in the vertical and horizontal motion of the vehicle. The accuracy of the vehicle model is highly dependent on the accuracy of the shock absorber model. The shock absorber is also one of the most non-linear and complex suspension system elements to model. There are two approaches to model shock absorbers: physical modeling based on physical and geometrical data, and nonparametric modeling based on experimental data. Each of them has particular advantages and disadvantages.

Manuscript received July 16, 2010.

Yan Cui is with the Beijing Institute of Technology, National Engineering Laboratory for Electric Vehicles, Beijing, 100081, China (phone: 864-320-0873; fax: 864-283-7208; e-mail: yanc@ clemson.edu).

Thomas R. Kurfess is with the Clemson University International Center for Automotive Research, 4 Research Drive, SC 29607 USA (e-mail: kurfess@clemson.edu).

Michael Messman is with the Clemson University International Center for Automotive Research, 4 Research Drive, SC 29607 USA (e-mail: MDMICAR@clemson.edu).

A. Physical Model of Shock Absorber

Physical models, which are based on a detailed description of the shock absorber's internal structure and ensuing dynamics during operation, describe the behavior in a large range of operating conditions very accurately (and are the most satisfactory ones from the theoretical point of view), but they are usually computationally complex, requiring time consuming computations when implemented in a full vehicle simulation. They contain several parameters whose values can only be determined by expensive measurements with special testing equipment. And even a small change of the shock absorber design may require an adjustment of the model and a new set of measurements, which in general can only be performed by the manufacturer of the shock absorber [4,5,6].

Lang developed a comprehensive physical damper model in 1977 [5]. This model includes approximately 80 parameters, is computationally complex, and is not suitable for comprehensive vehicle simulation studies or system identification. Later, Lang's model was condensed and validated by Morman [6]. Morman's model has been shown to be useful for studying the effects of design changes for a particular shock. Reybrouck developed a physical model with fewer parameters in 1994, valid for frequencies up to 20 Hz [7]. This model relied on semi-empirical coefficients, and did not consider the effect of internal modifications on damper performance. Talbott developed a model of an Öhlins NASCAR Nextel Cup shock in 2002 that considered the effect of damper tuning parameters, such as shim stack stiffness, shim stack preloads, and bleed orifice area on damper performance [8]. Emmons extended Talbott's model to include the head valve used in current Penske NASCAR Nextel Cup shocks [9].

B. Nonparametric Model of Shock Absorber

Nonparametric models establish a relationship between measured quantities, by purely mathematical means; the occurring parameters do not have a direct physical meaning. For the shock absorber, this is the relationship between the shock force and velocity. In this approach, a shock absorber is characterized by a 'black-box' system for a specific range of test conditions. In contrast to physical models, nonparametric models accurately describe the behavior of the system for a limited range of operating conditions that are tested. Furthermore, this approach yields computationally efficient models that can easily be adapted to a new set of test data.

A nonparametric model from experimental data using system identification techniques has been developed by Alanoly [10]. The model based on a restoring force surface

mapping has been developed [11]. The model considers the force to be a function of displacement and velocity. Although this model is limited to single frequency excitation, it serves as a useful tool for identifying nonlinearities in a system.

A comprehensive physical model of the shock absorber is necessary to study the effects of design changes and to tune the shock absorber to obtain the desired performance. However, if the objective is to characterize the performance of shock absorbers for full vehicle simulations, the nonparametric modeling approach is appropriate.

This paper develops three shock absorber models that can be quickly fit to experimental data and used for vehicle simulation. These models are based on the understanding that the shock absorber is predominantly a velocity-dependent device. The paper is organized as follows: in section II, a single-post shaker test bench is introduced and the experimental procedure for the shock absorber testing is described. In section III, three shock absorber models are presented and the models are validated via experimental data. In section IV, the influence of shock absorber models on vehicle vertical dynamics was analyzed. In section V, future opportunities for enhancing the shock models are discussed.

II. SHOCK ABSORBER TEST

A. Single-Post Shaker Test Bench

To develop a shock absorber model, the front shock absorber on the Mazda CX-7 was tested on a shock absorber test bench that was designed using a modified MTS single-post shaker, as shown in Fig. 1. A frame with an integrated load cell was built to mount the shock absorber. This test bench is actuated by a 40kN hydraulic cylinder, able of 10 inches of stroke. The system has excellent frequency response up to 80 Hz and velocities of 1.5 m/s.

The test bench is equipped with force, displacement and acceleration transducers. During the test, measurements of shock position, acceleration, and shock absorber force were recorded. The displacement was measured by a string pot and also a LVDT (Linear Variable Differential Transformer) that is installed on the single-post shaker.

It is widely known that shock absorber characteristics vary with temperature. To account for temperature effects, the shock absorber was instrumented with a thermocouple located on the outside of the main body of the shock absorber. The shock absorber was then excited and warmed up to 30°C prior to each test.

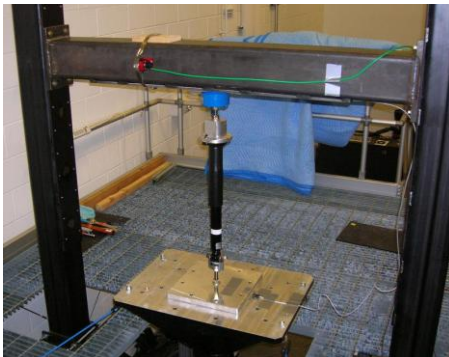


Fig. 1: Mazda CX-7 Shock Absorber on a Modified MTS Vibration Table

B. Data Acquisition

During each test, measurements of shock position, acceleration, shock force, and temperature were recorded at 2kHz using a SoMat eDAQ system, as shown in Fig. 2. The SoMat eDAQ is a portable stand-alone data acquisition system for testing in a wide range of environments. It has built in signal conditioning and the capability to perform a broad range of on-board data processing.

C. Shock Absorber Test Input Excitation

Tests on the single-post shaker are controlled by an MTS 407 controller. The controller allows for a wide variety of inputs, including sine waves, triangle waves and square waves. In this project, sinusoidal excitations with different amplitudes and frequencies were used to obtain the behavior of shock absorber at varying shock velocities. The input signals that were used during the test are shown in Table I. These values allow the shock absorber to work in the range of 0.01m/s to 1.3m/s, which correspond to typical velocities encountered by a vehicle suspension due to road irregularities.

The data for all the tests were extracted from the Infield eDAQ native) software format into LabVIEW for further analysis.

D. Shock Absorber Test Results

Test results of a sine wave input with 15mm amplitude at 15Hz are shown in Fig. 3. From the test results, the velocity dependent nature of the device is evident, validating the use of a force-velocity model.

From the data it is clear that the shock absorber force is a strongly nonlinear function of the piston velocity, and the behavior is not symmetrical with respect to velocity direction



Fig. 2: SoMAT eDAQ System used for the Shock Absorber Test

Table I: Summary of Sine Wave Inputs

Amplitude (mm)	Frequency (Hz)
5	30, 40, 50, 60
10	15, 20, 25, 30, 35
15	10, 15, 20, 25
20	5, 10, 15, 20
30	3, 5, 8, 10, 15
50	0.1, 0.5, 1, 1.5, 2, 3, 5, 10

(compression and rebound), as shown in Fig. 3(b). This nonlinearity makes the force in the rebound phase (when damper rod moves outwards from the damper body) greater than in the compression phase (when the damper rod moves into the damper body). From a design perspective this nonlinearity is important as it is used to optimize stability and comfort. Unfortunately, different values of damping force can be obtained with the same value of piston velocity showing an asymmetrical hysteretic phenomenon when conducting experiments on the shock absorber test bench, as shown in Fig. 3(b). In this paper, only the nonlinearity characteristics of the shock absorber will be modeled.

To reduce the influence of noise on the model fit, the force-velocity data from all tests were filtered using a low-pass filter with a cutoff frequency of 50Hz. The plot of the filtered force-velocity data is shown in Fig. 4.

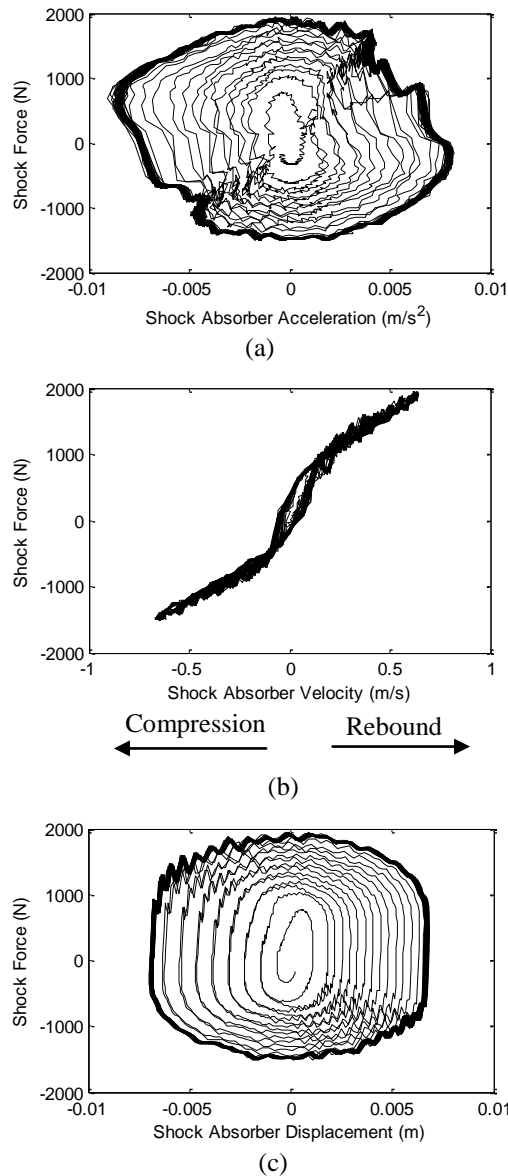


Fig. 3: Shock Absorber Test Result of Sine Wave input with 15mm amplitude at 15Hz

- (a) Plot of Force-Acceleration;
- (b) Plot of Force-Velocity;
- (c) Plot of Force-Displacement

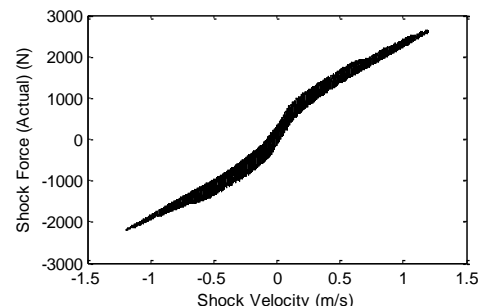


Fig. 4: Force-Velocity plot for Mazda CX-7 front shock

III. NONPARAMETRIC SHOCK ABSORBER MODELS

The force-displacement-velocity shock absorber model was discussed in [12]. However, if the model is validated with laboratory experiments from the shock absorber testing device only, the implementation of such a model into a full-vehicle simulation program for rough road investigations encounters a problem. During a rough road drive the shock absorber is utilized over its entire length of stroke, and occasionally the buffers are reached. The stroke of standard shock absorber testing machine is considerably shorter than that of the shock absorber, and even in cases when the length of stroke of the testing machine can be enlarged, it must be at least 3-4mm smaller than that of the shock absorber, to avoid possible damage to the testing machine. Thus, the region that is bounded by the trajectory for the maximum harmonic excitation frequency does not extend to the entire length of stroke of the shock absorber.[4]

For this research, the nonparametric force-velocity shock absorber behavior models which describe the relationship between shock velocity and force is developed using a least squares regression where shock velocity (v_s) is the independent variable and shock force (F_s) is the dependent variable. The model function has the form $f(v_s, \beta)$, where the vector β includes m adjustable parameters. β is adjusted to minimize the objective function, S , the sum of squared residuals, defined in equations (1) and (2).

$$r_i = F_i - f(v_s, \beta), i=1, \dots, m \quad (1)$$

$$S = \sum_{i=1}^n r_i^2 \quad (2)$$

Each of the model types are discussed in the ensuing text.

A. Linear Shock Absorber Model

This is the simplest model used in simulation-based analysis. It only considers linear behavior, as shown in (3).

$$F_s = cv_s \quad (3)$$

Using experimental data, the linear damping coefficient is identified. The force-velocity plot for linear shock absorber model is shown in Fig. 5.

B. Power Function Shock Absorber Model

The second choice for the shock absorber model is a simple power function, as shown in (4) and (5). For rebound

$$F(v) = q_1 v^{d_1} + l_1, \quad v \geq 0 \quad (4)$$

and, for compression

$$F(v) = q_2 (-v)^{d_2} + l_2, \quad v < 0 \quad (5)$$

The force-velocity plot for power function shock absorber model is shown in Fig. 6.

C. Segmented Polynomial Shock Absorber Model

Polynomials were used to fit the shock absorber in different velocity range. This method produced good fits with only 4th and 3rd order polynomials, as shown in (6) and (7). For rebound

$$F(v) = \begin{cases} a_{42}v^2 + a_{41}v + a_{40} & 0 < v \leq v_4 \\ a_{54}v^4 + a_{53}v^3 + a_{52}v^2 + a_{51}v + a_{50} & v > v_4 \end{cases} \quad (6)$$

and, for compression

$$F(v) = \begin{cases} a_{14}v^4 + a_{13}v^3 + a_{12}v^2 + a_{11}v + a_{10} & v \leq v_1 \\ a_{22}v^2 + a_{21}v + a_{20} & v_1 < v \leq v_2 \\ a_{34}v^4 + a_{33}v^3 + a_{32}v^2 + a_{31}v + a_{30} & v_2 < v \leq 0 \end{cases} \quad (7)$$

The force-velocity plot for polynomial shock absorber model is shown in Fig. 7.

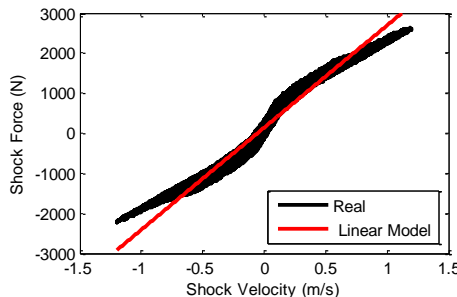


Fig. 5 Linear Shock Absorber Model

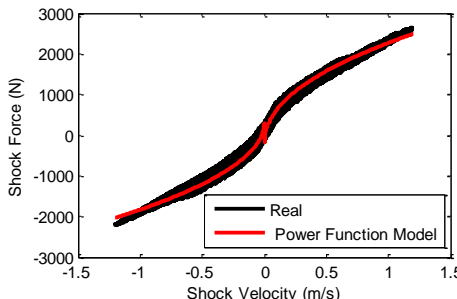


Fig. 6: Power Function Shock Absorber Model

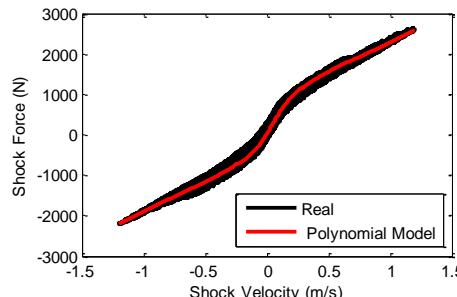


Fig. 7: Polynomial Shock Absorber Model

D. Model Validation

To validate the models, sinusoidal test data at various frequencies with a 30 mm amplitude was used. The model RMS errors are shown in Fig. 8. The power function and polynomial models capture the nonlinearity characteristics of shock absorber as is demonstrated by their significantly smaller RMS errors when compared to the linear model. The shock absorber forces of the models are compared with the experimental force in the time domain, as shown in Fig. 9. The close match between these two models and the experimental data demonstrate the high level accuracy of the models.

IV. QUARTER-CAR MODEL SIMULATION

The integration of the shock absorber model into full car model and being implemented and tested within the full car simulation in vertical direction is of main interest. However, prior to this step, the model should be tested with the simpler quarter-car model. Using the simpler quarter-car model, the enhanced shock absorber model's influence on the sprung mass vertical acceleration, a key comfort metric, can be evaluated.

In the quarter-car model, the suspension between the sprung mass and un-sprung mass is modeled using a spring element and a previously defined shock absorber model, as shown in Fig. 10. The representative parameter values for the quarter-car model simulation are shown in Table II. The random signal from 0.1 to 50Hz with the peak-to-peak value of 0.01m was used as road input to excite the quarter-car model, as shown in Fig. 11.

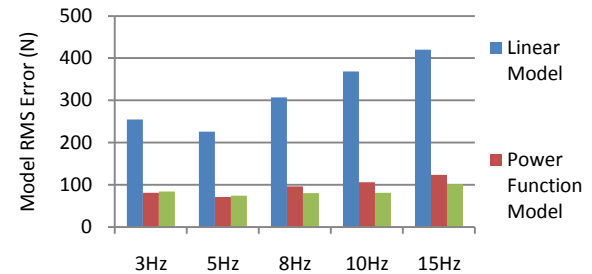


Fig. 8: Model RMS Error when shock absorber was excited by sine wave input with 30mm amplitude at different frequencies

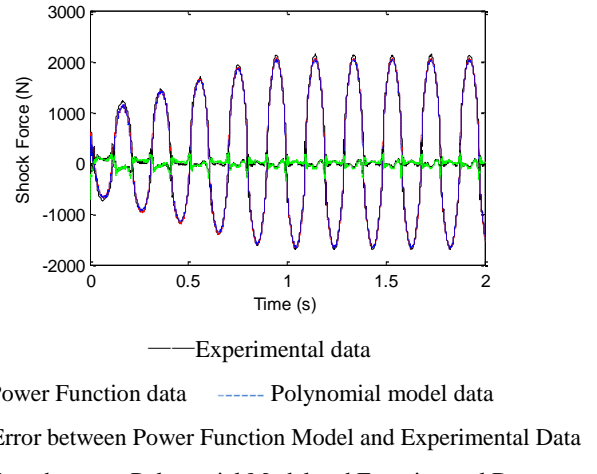


Fig. 9: Experimental, Power function and Polynomial Model Shock Absorber force (Sine wave input with 30mm amplitude at 5Hz)

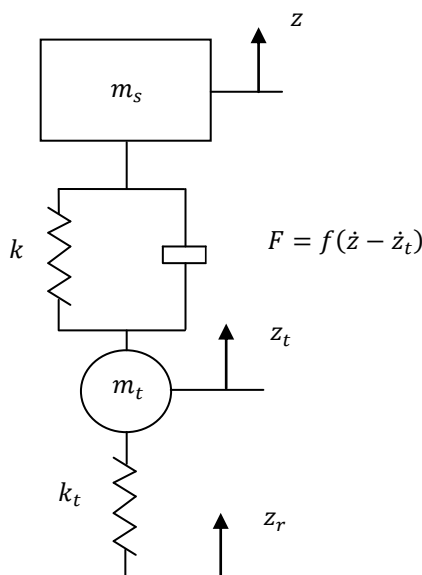


Fig. 10: Coupling of Quarter-car Model with Shock Absorber Model

Table II: Representative Parameter Values for Quarter-Car Model

m_s	Sprung mass	1200kg
m_t	Un-sprung mass	125kg
k	Suspension stiffness	60000 N/m
k_t	Tire stiffness	220000 N/m
c	Suspension damping	2500 Ns/m

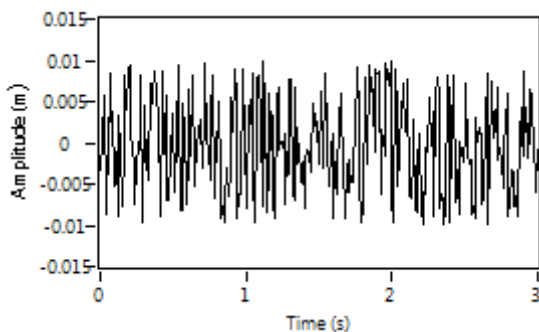


Fig. 11: Random Input Signal for Quarter-car Simulation

The frequency analysis of sprung mass acceleration shows the effect of shock absorber models on the dynamic behavior of the sprung mass. Fig. 12 shows the power spectral density of sprung mass acceleration for the three analyzed models. The polynomial and power function models had approximately the same peak values, but the linear model had a lower peak value except near 1 Hz which is likely to be the natural frequency of the sprung mass system.

With respect to time domain, the RMS of the sprung mass vertical acceleration of the linear model is 30% lower than the power function model. The difference between the power function model and the segmented polynomial model is less than 1%. Fig. 13 shows the sprung mass vertical acceleration

for the quarter-car model with three shock absorber models. Fig. 14 shows the evaluation of the damping force for three shock absorber models. These two figures confirm that the power function model and polynomial model demonstrated similar behaviors, and linear model deviated significantly.

V. CONCLUSION AND FUTURE WORK

This paper has summarized the work to develop two efficient empirical nonlinear models for a shock absorber. The models were created and validated using experimental data generated from a single-post shaker test bench. The influence of shock absorber models on a vehicle's vertical dynamic behavior has been analyzed. The simulation results show that the two nonlinear models demonstrated similar behaviors.

It was found that the power function model and polynomial model had less than 100 N RMS error over a wide range of operating conditions. The error was larger at high frequencies because of the hysteretic characteristics of the shock absorber. The validation results suggested that a lag should be added to the model at high frequency to capture the characteristic hysteresis of the shock absorber. The shock absorber model that can capture the nonlinear properties and hysteresis characteristics of the shock absorber will be integrated into full vehicle simulation in vertical direction.

REFERENCES

- [1] M. C. Smith, "Achievable Dynamics Response for Automotive Active Suspension," Vehicle System Dynamics, vol. 1, pp. 1-34, Jan. 1995
- [2] H. Peng, R. Stranahan and A. G. Ulsoy, "A Novel Active Suspension Design Technique Simulation and Experimental Results," Proc. of American Control Conference, June 1997.
- [3] W. Gao, N. Zhang, J. Dai, "A stochastic quarter-car model for dynamics of vehicles with uncertain parameters," Vehicle System Dynamics, vol. 46, No.12, pp. 1159–1169, December 2008.
- [4] M. Weigel, W. Mack, and A. Riepl, "Nonparametric shock absorber modelling based on standard test data," Vehicle System Dynamics, 2002. 38(6): p. 415-432.
- [5] H. Lang, "Automotive Dampers at High Stroking Frequency," 1977, University of Michigan.
- [6] K. Morman, "A model for the Analysis and Simulation of Hydraulic Shock Absorber Performance, Part I - Theoretical Development (SR-83-043), Part II - Parameter Identification and Model Validation Studies (SR-86-61)," in Ford Motor Company Research Staff Reports.
- [7] K. Reybrouck, "A Nonlinear Parametric Model of an Automotive Shock Absorber," SAE paper No. 940869.
- [8] M. Talbot, and J. Starkey, "An Experimentally Validated Physical Model of a High-Performance Mono-Tube Damper," SAE paper No.2002-01-3337.
- [9] S. Emmons, B. Boggs, and M. Ahmadian, "Parametric Modeling of a High-Adjustable Race Damper," in ASME International Mechanical Engineering Congress and Exposition. 2006.
- [10] J. Alanoly, P. Kuber, C. Rubio-Ratton, "Large Deflection Non-linear Component Models for Durability Simulation," Proc. 7th Worldwide Vehicle Dynamics Conference. Ford Motor Co., Dearborn, MI, Oct. 1993
- [11] G. Belingardi and P. Campanile, "Improvement of the Shock Absorber Dynamic Simulation by the Restoring Force Mapping Method," Proc. of the 15th International Seminar on Model Analysis and Structural Dynamics. Leuven, Belgium, pp.441-454,1990
- [12] R. Basso, "Experimental Characterization of Damping Force in Shock Absorbers with Constant Velocity Excitation," Vehicle System Dynamics 30 (1998), pp.431-442.

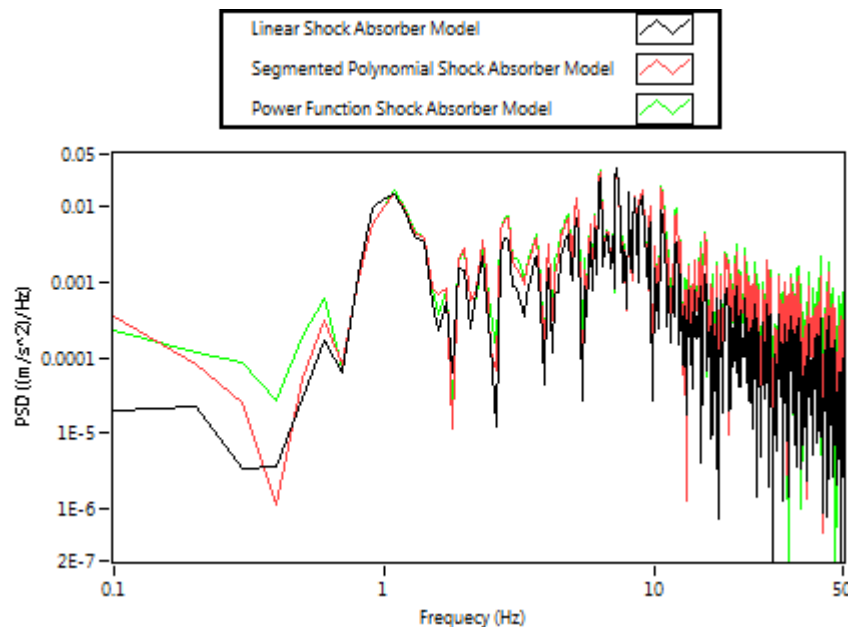


Fig. 12: Power Spectral Density (PSD) of the Sprung mass Acceleration

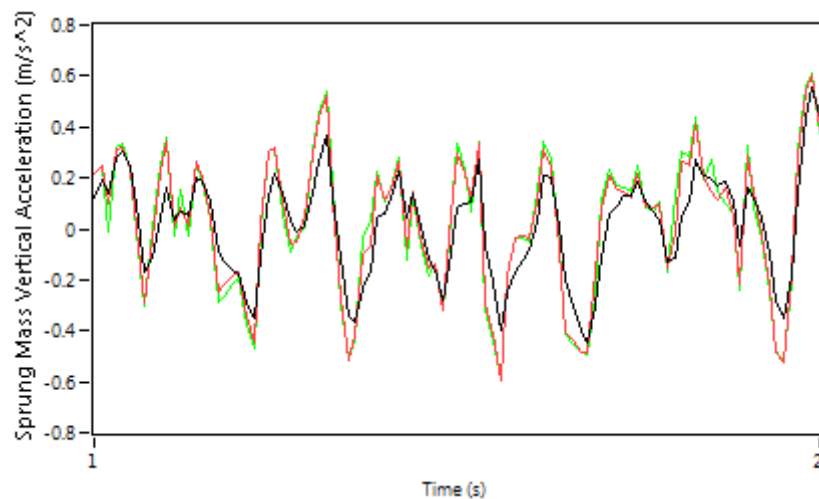


Fig. 13: Sprung Mass Vertical Acceleration of Random Road Input

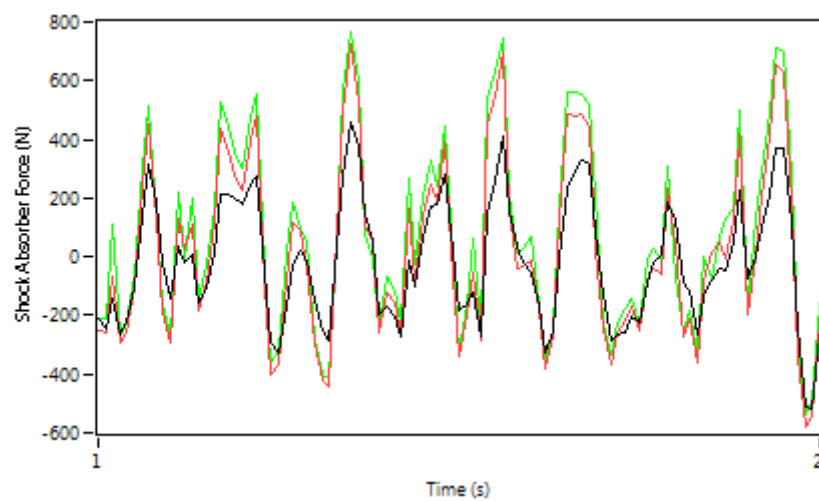


Fig. 14: Shock Absorber Force